Experimental studies of enhanced Raman scattering from a hexagonally poled $LiTaO_3$ crystal

P. Xu, S. N. Zhu,* X. Q. Yu, S. H. Ji, Z. D. Gao, G. Zhao, Y. Y. Zhu, and N. B. Ming
National Laboratory of Solid State Microstructures, Nanjing University, Nanjing, 210093, China
(Received 10 May 2005; published 31 August 2005)

The study of phonon-polariton Raman scattering continues to be a challenge, in part because of the difficulty of measuring relatively low intensity of scattered signals. This paper reports the experimental results on phonon-polariton Raman scattering in a hexagonally poled $LiTaO_3$ crystal, showing the anti-Stokes and Stokes Raman signal intensities are significantly enhanced by cascading a couple of quasi-phase-matching processes where the coherent polariton fields are driven and the enhanced scattering signals are further amplified.

DOI: 10.1103/PhysRevB.72.064307 PACS number(s): 78.30.−j, 42.65.Dr, 42.65.Ky, 71.36.+c

Quasi-phase-matching (QPM) makes nonlinear light wave mixing active in a more general stage through phase compensation with the modulation of secondorder nonlinear susceptibility $\chi^{(2)}$ of the medium,[1–3] which usually leads to generating laser at a new frequency efficiently by sum frequency,[4] difference frequency,[5] or parametric amplification.[6] In addition, the QPM approach has promising applications, by modulating the phase and amplitude of an optical field,[7] compression of a tunable-chirp pulse,[8] generation of an optical soliton,[9] realization of optical bistability,[10] optical chaos,[11] etc. Other progresses, such as use of QPM material as a coherent THz radiation source[12] and bright entanglement pair source,[13] have emerged.

In addition, the QPM approach can also enhance the scattering signal intensity in a nonlinear medium. In a recent work,[14] we reported the generation of a conical second-harmonic beam in a hexagonally poled $LiTaO_3$ (HPLT) crystal by a quasi-phase-matched frequency adding of incident light and elastic scattering light. The information relating to elastic scattering in the HPLT as well as its symmetry was revealed from the nonlinear diffractive pattern. QPM, for the first time, showed its elegant function in the study of light scattering.

Raman scattering, as a sort of inelastic scattering, is always accompanied by frequency change. Raman scattering can be mediated by many different types of elementary excitations in a medium, such as TO phonons, phonon-polaritons, or plasmons. Compared to elastic scattering, Raman scattering is much weaker, so it brings more challenge in detection. One immediate question can be proposed, that is, whether Raman scattering is possibly enhanced by the QPM process in a $\chi^{(2)}$ modulated medium and what spectrum characteristic may be revealed if this occurs. In this paper, we will report the experiment studies on QPM-enhanced phonon-polariton (P-P) Raman scattering in a manual microstructure—a HPLT crystal. The QPM approach was first operated to generate two laser beams to drive an intense coherent P-P field in the HPLT crystal and was then used to amplify the generated Raman signals by parametric amplification, which resulted in the generation of a stimulated P-P Raman scattering. The anti-Stokes and Stokes spectrum with very low Raman shift down to 2 cm^{-1} and very high scattering order up to the 11th rank was detected from the medium. The resulting spectrum exhibits a comb-shaped structure with an equal frequency interval tunable by changing the frequency of excited polariton. The QPM approach was successfully introduced into the $\chi^{(2)}$ medium for enhancement of inelastic scattering.

In experiment, the HPLT slice of 20 mm(x) × 15 mm(y) × 1 mm(z) was fabricated by a field poling technique.[15] The nearly circularly inverted domains have $-\chi^{(2)}$ distributed hexagonally in the $+\chi^{(2)}$ background, "lattice parameter" a = 9.05 μm, and a reversal factor $D = \sim 23\%$. This structure offers a reciprocal vector $|G| = 4\pi/\sqrt{3}a$ along the x axis, which is of sixfold symmetry. Figure 1 is the experimental setup. The laser source is a tunable optical parametric oscillator (OPO), which can supply tunable pair beams generated through down-conversion from a 355 nm laser. During this measurement, one beam was tuned at wavelength of around 1064 nm as signal, the other one dependently tuned around 532 nm as pump λ_0. The pair beams have nearly Gaussian profiles with a pulse width of ~5 ns, linewidth ≤0.1 cm^{-1}, and repetition rate of 10 Hz, and were linearly polarized along the z axis of the crystal. Two lenses, of focal lengths f = 40 cm and f = 20 cm, were used to focus the pump and signal beams into the sample with beam divergences of 10 and 16 mrad, respectively.

The pump and signal beams from the OPO were incident onto the HPLT sample and propagated along its x axis, which resulted in the generation of the third laser beam also at a wavelength of a round 1064 nm by the difference frequency generation (DFG) process. The reciprocal G by $\chi^{(2)}$ modulation along the x axis made this process quasi-phase-matched. Conventionally, in $LiTaO_3$ crystal the lowest A_1 phonon mode (200 cm^{-1} or so) (Ref. 16) and the corresponding phonon-polariton lying on its low-frequency wing can all be excited but rather weak if only a single laser beam is used. In

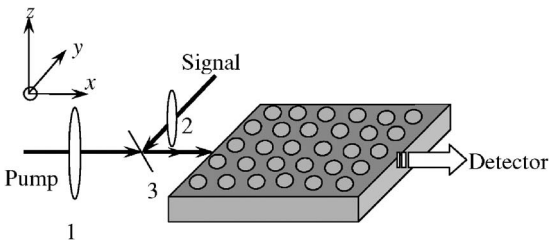

FIG. 1. Experimental setup in which 1 and 2 are focal lens and 3 is the mirror of high reflection for signal and high transmission for pump at 45°.

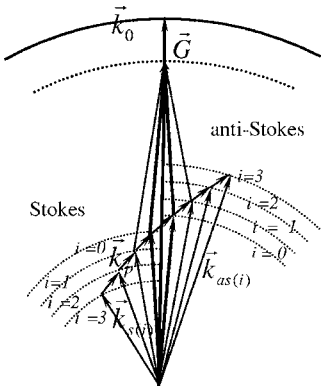

FIG. 2. Phase matching in the cascaded generation of anti-Stokes and Stokes Raman signals. Only the first three orders are sketched for simplification. The inner momentum parallelogram accounts for the initial QPM-DFG process and the outer one for the QPM parametric amplification for anti-Stokes and Stokes signals.

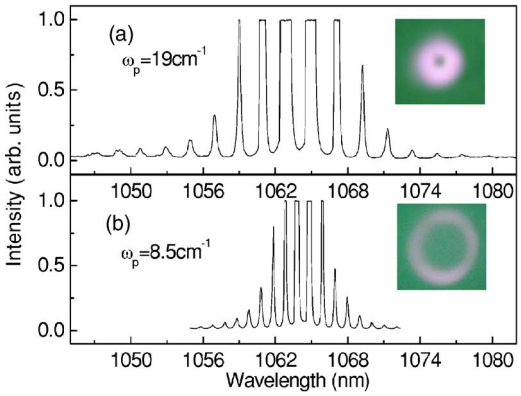

FIG. 3. (Color online) Raman spectra with (a) $\omega_p=19$ cm^{-1} and $\lambda_0=531.82$ nm and (b) $\omega_p=8.5$ cm^{-1} and $\lambda_0=531.92$ nm. The insets are the corresponding spatial distributions.

the experiment, however, the excitation was greatly improved. The intense P-P field (k_p,ω_p) was driven coherently by two laser beams, k_1 and k_2, under the conservation conditions of wave vector and energy:

$$k_p = k_1 - k_2 \quad \text{and} \quad \omega_p = \omega_1 - \omega_2. \tag{1}$$

Henceforth we define $k_1(k_2)$ as the higher(lower) frequency beam between the signal and the difference frequency beams. Experimentally, $k_p=k_1-k_2$ could be satisfied by making use of the divergence of k_1 and k_2.

The intense P-P fields then supplied the inelastic source and brought about new additional frequency $\omega_{as_{(n)}}=\omega_1+n\omega_p$ at anti-Stokes and $\omega_{s_{(n)}}=\omega_2-n\omega_p$ at Stokes, where $n=1,2,3$, standing for the order of Raman scattering. Meanwhile the wave vector conservation demands

$$k_{as_{(n)}} = k_{as_{(n-1)}} + k_p \quad \text{and} \quad k_{s_{(n)}} = k_{s_{(n-1)}} - k_p. \tag{2}$$

Here $k_{as_{(n)}}$ and $k_{s_{(n)}}$ are the wave vectors of the nth-order anti-Stokes and Stokes, respectively, and for generation of the first-order Raman pair $k_{as_{(1)}}$ and $k_{s_{(1)}}$, we define $k_{as(0)}=k_1$ and $k_{s(0)}=k_2$. Equation (2) can be ensured since the crossing angle of $k_{as_{(n)}}$ to $k_{as_{(n-1)}}$ is rather small compared with the divergence of k_1 and k_2. Equations (1) and (2) can therefore be combined to be a cascaded automatic-phase-matching (APM) two-step $\chi^{(2)}$ process. Figure 2 is the sketched momentum geometry of this cascaded process. Owing to an intense coherent P-P field being excited, the high-order scattering occurred. The Raman spectra exhibited a multi-peak structure with $2(n+1)$ separate frequencies with an equal frequency interval and the spatial distribution of the scattering light on the screen behind the sample presented a round spot or a round ring, depending on the phase-matching geometry of the foregoing QPM-DFG process. If the pump wavelength exceeds 531.64 nm, DFG must be noncollinear, i.e., the generated k_1 and k_2 are not along the direction of pump k_0 but construct a momentum triangle. Then a ring pattern can be expected on screen and the sequential APM two-step process occurred also within the ring. Experimentally the pattern developed from an obscured spot to a ring when the wavelength of pump k_0 varied from 531.64 to 532.39 nm, which was very consistent with theoretical estimation. In this experiment, the coherent P-P field was tuned in the range of 2–42 cm^{-1} by changing pump wavelength, which lay on the low-frequency wing of the lowest A_1-TO phonon mode. Although the P-P dispersion characteristic may still be disturbed by possible Debye relaxation mode, defect mode, or other low-frequency excitations in this crystal, the previous work gave that absorption coefficients of the polariton in this range were small, showing the polariton here to be photon-like.[17]

The Raman spectra corresponding P-P frequency $\omega_p=19$ and 8.5 cm^{-1} are shown in Figs. 3(a) and 3(b), respectively. The insets are their output patterns distributed on the screen. The spectra have nearly symmetric distribution in which k_1, k_2 (the middle two peaks) exhibit almost identical intensity due to QPM interaction. The peaks are where the anti-Stokes or Stokes side has an order number of as many as 7 or 8. The intensity of high order Raman signal is relatively low but decreases more slowly with n getting larger. In Fig. 3(a) the anti-Stokes side, the intensity ratio of adjacent peaks $I_{as(n)}/I_{as(n-1)}$ differs greatly, from 14% $(n=1)$ to 70% $(n=8)$. The measured average power for the highest order of Raman shift was 100 nW or so under the pump power of 4 mW and the power of k_1 or k_2 of 10^{-2} mW. All peaks had almost the same bandwidth to be 0.15 nm limited by the spectrometer resolution of about 1.5 cm^{-1}.

The intensity of these Raman peaks generated by the cascaded process was essentially related with the equivalent nonlinear susceptibility $\chi_p^{(3)}$ that was defined: $\chi_p^{(3)}=4\pi\omega_p\chi_1^{(2)}\chi_2^{(2)}/cn_p\alpha_p^2$,[18] in which $\chi_1^{(2)}=(1-2D)\chi^{(2)}\times(-\omega_p;\omega_1,-\omega_2)$, $\chi_2^{(2)}=(1-2D)\chi^{(2)}(-\omega_{as(n)};\omega_{as(n-1)},\omega_p)$, α_p is the polariton absorption coefficient, n_p is the refraction index of polariton, and c is the light velocity in vacuum. Both $\chi_1^{(2)}$ and $\chi_2^{(2)}$ are in proportion to $\chi^{(2)}$ of crystal and structure-sensitive dependent on the reversal factor D of domain modulation, which distinguishes QPM material from homogeneous crystal. Experimentally, we did observe the dependence of Raman intensity on the parameter D. Besides,

the direct four-wave-mixing (FWM) relating to third-order nonlinear susceptibility $\chi_d^{(3)}$ of the medium could also contribute to the multi-order Raman signal by fulfilling $k_{as(n)}=2k_{as(n-1)}-k_{as(n-2)}$ and $k_{s(n)}=2k_{s(n-1)}-k_{s(n-2)}$. But $\chi_d^{(3)}$ was much smaller than $\chi_p^{(3)}$ in our case because of the phonon-polariton excited here far from the resonance of A_1 mode.[18]

In a traditional P-P Raman experiment, Raman signal was very weak compared with incident beams and brought challenge in detection. Experiment with nanosecond pulse in GaP gave a relative intensity of $10^{-7}-10^{-6}$,[19] 10^{-3} in calcite with picosecond pulse,[20] also 10^{-3} in $LiNbO_3$ even though femtosecond pulse was used.[21] Meanwhile a single $\chi^{(3)}$ process such as stimulated Raman scattering (SRS) and a direct FWM, which was realized in fiber[22] or cavity,[23] gave the prevalent value of $10^{-5}-10^{-3}$ with pico- or nanosecond pulse; other cases gave a little larger conversion efficiency only if femtosecond pump was used[24] or the medium was of high Raman activity such as liquid or gas.[25] These experimental values were in good approximation with theoretical estimation by the relevant $\chi_p^{(3)}$ or $\chi_d^{(3)}$ mentioned above. So in our case with nanosecond pulse and performing at frequency far from phonon resonance, the relative intensity of 14%–70% and the scattering order up to 8 should be attributed to the subsequent QPM parametric amplification process. It could bring the rapid growth of the seed signal.[26] Here the seed was the generated anti-Stokes and Stokes signals and k_0 serves as the pump. Then

$$k_0 = k_{as_{(n)}} + k_{s_{(n)}} + G \quad \text{and} \quad \omega_0 = \omega_{as(n)} + \omega_{s(n)}, \tag{3}$$

$n=1,2,3\ldots$. In fact, setting $n=0$ this equation can also describe the initial QPM-DFG process producing the two coherent fields k_1 and k_2, which is shown by the inner momentum parallelogram in Fig. 2 while the outer one stands for the parametric amplification process of $n\neq 0$. Therefore the amplitudes of each order anti-Stokes $E_{as(n)}$ and Stokes $E_{s(n)}$ should develop according to the coupling equations below:

$$\frac{dE_{as(n)}}{dx} = -i\frac{\omega_{as(n)}}{n_{as(n)}c}(f_{as(n)}\chi_p^{(3)}E_{as(n-1)}E_1E_2^* + \chi_{eff}^{(2)}E_0E_{s(n)}^*),$$
$$\frac{dE_{s(n)}}{dx} = -i\frac{\omega_{s(n)}}{n_{s(n)}c}(f_{s(n)}\chi_p^{(3)}E_{s(n-1)}E_2E_1^* + \chi_{eff}^{(2)}E_0E_{as(n)}^*), \tag{4}$$

in which E_0 was assumed to be constant since less than 5% of the pump was depleted experimentally. E_1 and E_2 were the amplitudes of k_1 and k_2, respectively; $\chi_{eff}^{(2)}=f\chi^{(2)}\times(-\omega_{as(n)};\omega_0,\omega_{s(n)})/2$ was effective nonlinear susceptibility for this parametric amplification process. Here $f=0.29$ was the Fourrier coefficient of reciprocal G; $n_{as(n)}$ and $n_{s(n)}$ were the refraction indexes; and $f_{as(n)}$ and $f_{s(n)}$ were spatial factors which were related with polariton's linear diffraction effect and its spatial overlap with related parametric waves.[26] The coupling equations are under proper approximation, such as the multi-polariton process, are not included because it involves higher order nonlinear susceptibility. So the APM two-step process expressed by the first term on the right-hand side of Eq. (4) was the main origination of the Raman signal. The second term described the amplification process of anti-Stokes and Stokes signals by pump. The traditional P-P Raman scattering through a two-step process can also be described by Eq. (4) but without the amplification term, so the intensity was rather weak. Exact numerical simulation of Eq. (4) was a little complicated due to the difficulty of the selection of several parameters, here for simplicity, we omitted the first term and substituted just a proper initial seed $I_{as(n)}(0)$ for the optical amplification process. Then we got the anti-Stokes intensity gain at its low limit, which is similar to the case in a traditional parametric process[27] and it is

$$G_{as(n)}(l) = \left(\frac{I_{as(n)}(l)}{I_{as(n)}(0)} - 1\right) \propto \frac{2\omega_{as(n)}\omega_{s(n)}\mu_0(\chi_{eff}^{(2)})^2}{n_0 n_{as(n)} n_{s(n)}\varepsilon_0 c^3} I_0 l^2, \tag{5}$$

where l is the interaction length, n_0 is the refraction index of pump wave, and ε_0 and μ_0 are the vacuum permittivity and susceptibility, respectively. $G_{as(n)}(l)$ is proportional to pump intensity I_0 and the square of l. In experiment, we measured the dependence of the Raman spectrum on the pump power, under the condition that k_1 and k_2 were adjusted to identical intensity, so the seed $I_{as(n)}(0)$ decided by the origination term in Eq. (4) was kept identical. Figures 4(a) and 4(b) reveal great differences both in scattering intensity and scattering order with moderate pump powers of 3.0 and 8.2 mW, respectively. The inset demonstrated that the intensity of the first-order anti-Stokes signal increased linearly with pump power, which can be deduced from Eq. (5). Moreover, an exponential growth can be expected if higher power pump is used.[26] Nevertheless, using the present model we cannot explain exactly the intensity ratio $I_{as(n)}/I_{as(n-1)}$, which increases with n from 14% ($n=1$) to 70% ($n=8$) in Fig. 3(a). We suggest a possible explanation that the high-order peaks can be produced through the several direct FWM processes. A richer variety of such phase-matching geometries appear for larger n, thus corrections should be made to the origination

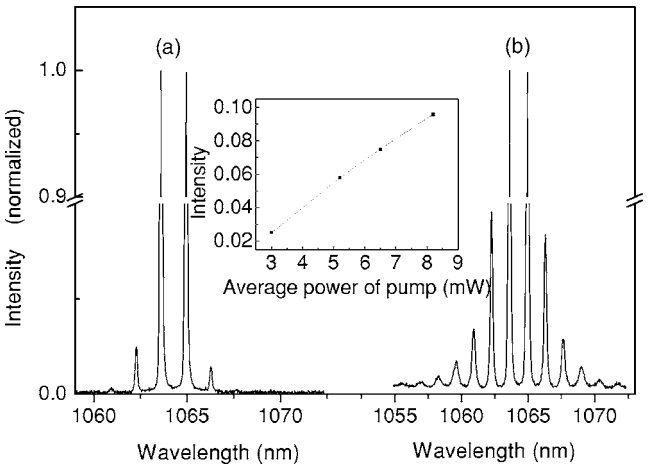

FIG. 4. Raman spectra with different pump intensities at $\lambda_0=531.89$ nm. Average pump powers in (a) and (b) are 3.0 and 8.2 mW, respectively. The inset is the first anti-Stokes intensity going linearly with pump intensity.

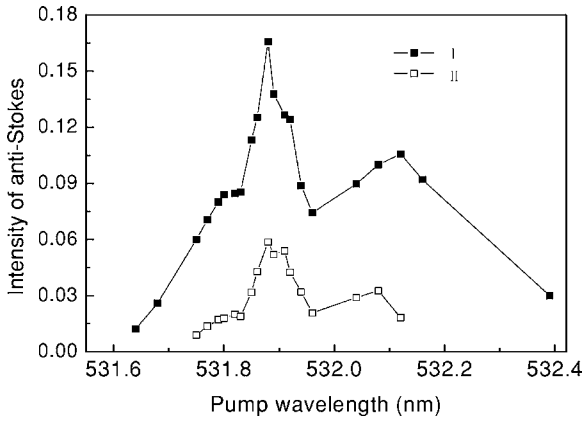

FIG. 5. The first- (I) and second- (II) order anti-Stokes intensity relative to the intensity of k_1 when pump wavelength varies.

term in Eq. (4) especially when n gets much larger.

We varied the wavelength of pump λ_0 in the range of 531.64–532.39 nm and observed the accompanied Raman spectra are similarly distributed but the intensity differs, especially at some pump wavelength the scattering order is up to 11. Figure 5 displays the first- and second-order anti-Stokes signal intensity dependent on λ_0 by plots I and II, respectively. Both exhibit two maximums. This can be attributed mainly to the difference in the process the Raman signal originated: as λ_0 tuned toward 531.64 nm (collinear QPM-DFG) or neared 532.39 nm (maximal permissive wavelength for noncollinear QPM-DFG), the parametric interaction volume got to be smaller and this significantly decreased the DFG efficiency and accordingly decreased the generation of phonon-polariton and the intensity of the final Raman signal. When λ_0 neared 532 nm, the frequency of excited phonon-polariton was very low due to k_1 and k_2 being nearly degenerate. The diffraction effect got rather remarkable, which led $\chi_p^{(3)}$ contribution diminish sharply.[26] Thus plots in Fig. 5 should contain two maximums. All the higher-order peaks follow the same rule as shown in Fig. 5, except that they have lower intensity.

In our experiment range, a low-frequency polariton in the range of 2–42 cm^{-1} was excited, which corresponded to a popular region of THz.[12] We did not find obvious evidences for low-frequency local excitation in this range, which consisted with most of the previous works.[14] Although the polariton in this range is photon-like, the two-step $\chi^{(2)}$ process, in some meaning, still differs from a general optical parametric process occurring in the visible and infrared ranges of medium. In fact, the polariton has a short free path varying from several millimeters to several centimeters due to damping,[19] which made the process not so efficient compared to a general cascaded $\chi^{(2)}$ process.

It is worth noting the P-P Raman signal here is crucially dependent on the reversal factor D. As $D \rightarrow 0.5$, $\chi_p^{(3)} \rightarrow 0$; the Raman signal only originates from direct FWM because $\chi_d^{(3)}$ always exists. In this case, the Raman signal can still be amplified by the later QPM parametric process. However, it is relatively weak compared with the present result because $\chi_d^{(3)} \ll \chi_p^{(3)}$ when ω_p is far away from that of the A_1 mode. We proved the presumption from a one-dimensionally periodically poled $LiTaO_3$ with $D \rightarrow 0.5$. In the present work we used a two-dimensional structure instead of a one-dimensional structure since the former has a better homogeneity of poling usually and can be well controlled for a required parameter D.

In summary, the P-P Raman scattering was experimentally studied in a HPLT crystal. In contrast to a single domain $LiTaO_3$ crystal, the HPLT crystal offers a valuable platform to perform QPM interaction. In this work, the QPM structure was used for a dual purpose: to assist in exciting intense polariton fields first and then to amplify the enhanced Raman signal. A simplified step-accomplished model has been proposed to describe the cascaded nonlinear processes and a set of coupling equations is developed to account for the experiment results. The resulting Raman spectrum exhibited a comb-shaped structure with high intensity, suggesting it may be of technological importance for developing a novel Raman laser with the multi-wavelength output and a tunable frequency interval. The work presents a novel and efficient method to study the inelastic scattering and the elementary excitation in a nonlinear medium.

We thank H. T. Wang, J. L. He, G. X. Chen, and A. Hu for valuable discussions and J. Sun for help during this experiment. This work is supported by grants from the National Advanced Materials Committee of China and the State Key Program for Basic Research of China (2004CB619003), and by the National Natural Science Foundation of China under Contract No. 90201008.

*Corresponding author. Email address: zhusn@nju.edu.cn

[1] J. Armstrong, N. Bloembergen, J. Ducuing, and P. S. Pershan, Phys. Rev. **127**, 1918 (1962).
[2] P. A. Franken and J. F. Ward, Rev. Mod. Phys. **35**, 23 (1963).
[3] V. Berger, Phys. Rev. Lett. **81**, 4136 (1998).
[4] S. N. Zhu, Y. Y. Zhu, and N. B. Ming, Science **278**, 843 (1997).
[5] A. Chowdhury, S. C. Hagness, and L. McCaughan, Opt. Lett. **25**, 832 (2000).
[6] M. A. Arbore and M. M. Fejer, Opt. Lett. **22**, 151 (1997).
[7] D. K. Serland, P. Kumar, M. A. Arbore, and M. M. Fejer, Opt. Lett. **22**, 1497 (1997).
[8] A. M. Schober, G. Imeshev, and M. M. Fejer, Opt. Lett. **27**, 1129 (2002).
[9] C. B. Clausen, O. Bang, and Y. S. Kivshar, Phys. Rev. Lett. **78**, 4749 (1997).
[10] B. Xu and N. B. Ming, Phys. Rev. Lett. **71**, 1003 (1993).
[11] K. N. Alekseev and A. V. Ponomarev, JETP Lett. **75**, 174 (2002).
[12] Y. Sasaki and A. Yuri, Appl. Phys. Lett. **81**, 3323 (2002).
[13] M. J. A. de Dood, W. T. M. Irvine, and D. Bouwmeester, Phys. Rev. Lett. **93**, 040504 (2004).

[14] P. Xu, S. H. Ji, S. N. Zhu, X. Q. Yu, J. Sun, H. T. Wang, J. L. He, Y. Y. Zhu, and N. B. Ming, Phys. Rev. Lett. **93**, 133904 (2004).
[15] S. N. Zhu, Y. Y. Zhu, Z. Y. Zhang, H. Shu, H. F. Wang, J. F. Hong, and C. Z. Ge, J. Appl. Phys. **77**, 5481 (1995).
[16] A. F. Penna, A. Chaves, P. da R. Andrade, and S. P. S. Porto, Phys. Rev. B **13**, 4907 (1976).
[17] G. P. Wiederrecht, T. P. Dougherty, L. Dhar, D. E. Leaird, K. A. Nelson, and A. M. Weiner, Phys. Rev. B **51**, 916 (1995).
[18] G. Kh. Kitaeva, A. A. Mikhailovsky, P. S. Losevsky, and A. N. Penin, Opt. Commun. **138**, 242 (1997); G. Kh. Kitaeva, K. A. Kuznetsov, A. A. Mikhailovsky, and A. N. Penin, J. Raman Spectrosc. **31**, 767 (2000).
[19] J. P. Coffinet and F. De Martini, Phys. Rev. Lett. **22**, 60 (1969).
[20] R. R. Alfano and S. L. Shapiro, Phys. Rev. Lett. **26**, 1247 (1971).
[21] P. C. M. Planken, L. D. Noordam, J. T. M. Kennis, and A. Lagendijk, Phys. Rev. B **45**, 7106 (1992).
[22] A. V. Husakou and J. Herrmann, Appl. Phys. Lett. **83**, 3867 (2003).
[23] V. Pasiskevicius, A. Fragemann, and F. Laurell, Appl. Phys. Lett. **82**, 325 (2003).
[24] D. A. Akimov, E. E. Serebryannikov, and A. M. Zheltikov, Opt. Lett. **28**, 1948 (2003).
[25] H. Kawano, T. Mori, Y. Hirakawa, and T. Imasaka, Opt. Commun. **160**, 277 (1999).
[26] Y. R. Shen, *The Principles of Nonlinear Optics* (Wiley, New York, 1984).
[27] R. L. Byer, J. Nonlinear Opt. Phys. Mater. **6**, 549 (1997).